NANOSYSTEMS: PHYSICS, CHEMISTRY, MATHEMATICS, 2017, 8 (5), P. 647–653

Peculiarities of $LaFeO_3$ nanocrystals formation via glycine-nitrate combustion

A. Bachina[1,2], V. A. Ivanov[1], V. I. Popkov[1,2]

[1]Saint Petersburg State Technological Institute (Technical University),
Moskovskiy 26, St. Petersburg, 190013, Russia

[2]Ioffe Institute, Russian Academy of Sciences,
Politekhnicheskaya 26, St. Petersburg, 194021 Russia

a.k.bachina@gmail.com

PACS 81.07.-b **DOI 10.17586/2220-8054-2017-8-5-647-653**

Varying glycine to nitrate ratio in the initial solution the powders based on nanocrystalline $LaFeO_3$ were synthesized by solution combustion synthesis. The powders were studied by X-ray diffractometry, scanning electron microscopy, adsorption analysis and helium pycnometry. The average crystallite size of the synthesized $LaFeO_3$ nanocrystals ranged from 18±2 to 85±9 nm, and the specific surface area of the nanopowders based on them ranged from 8 to 33 m^2/g. Based on the results, the influence of redox composition of the reaction solution on the nature of the combustion processes, as well as the composition, structure and properties of $LaFeO_3$ nanocrystals were analyzed. Here, it was shown, that the nanopowders have specific microstructure in terms of monocrystalline nanoscale layers of lanthanum orthoferrite, therefore it is allowed to consider them as a promising base for catalytically and magnetically functional materials.

Keywords: lanthanum orthoferrite, glycine-nitrate combustion, nanocrystals, formation mechanism, XRD, SEM.

Received: 15 September 2017

Revised: 9 October 2017

1. Introduction

Lanthanum orthoferrite is one of the rare-earth orthoferrites which has perovskite-like structure and crystallizes within the orthorhombic crystal system (*Pbnm* space group) [1]. Lanthanum orthoferrite, due to its wide prevalence in comparison with other rare-earth elements (REE) and its particular property set, is the basis for many functional materials applied in catalysis, solid-oxide fuel cells, chemical sensors, magnetic and electrode devices etc. [2–9]. Lately, materials based on $LaFeO_3$ are also considered as promising materials to obtain hydrogen by the photocatalytic decomposition of water under visible light irradiation [10–12]. In this case, the efficiency and the rate of H_2 generation are defined by the value of a specific surface area of photocatalyst and therefore the use of nanoscale lanthanum orthoferrite powders can be more advantageous relative to coarse-crystalline ones.

Nanocrystals of lanthanum orthoferrite and other rare-earth orthoferrites are conventionally obtained by soft chemistry methods: sol-gel synthesis [13, 14], hydrothermal synthesis [15–17], thermal treatment of precursors with different chemical composition [18, 19] and others [20]. In the most cases, the crystallite size and the specific surface area of successfully obtained $LaFeO_3$ nanocrystals are about 50 nm and 10 m^2/g, correspondingly. However, to use materials based on lanthanum orthoferrite in real photocatalytic processes the value of crystallite size should be rather smaller.

Recently, the solution combustion method has been actively developed to obtain nanocrystalline oxides. The method is based on redox reaction, which occurs during the thermal treatment of solutions containing the respective metal nitrates and an organic reducing agent, for example, glycine, citric acid, urea, etc. The reaction is accompanied by enormous heat release which supports the process autonomously after combustion initiation by an external heating source. As a rule, the result of the reaction is the formation of single-phase oxide nanopowders with a high specific surface area and small crystallite size. Thus, application of this synthesis approach seems to be highly reasonable and promising.

However, since the formation of the nanocrystalline oxides under the described conditions is a rather complicated combination of physical-chemical processes, the particular properties of nanopowders, in general, depend on different factors including the composition of a reaction mixture, material and shape of a reactor, composition of media, under which the synthesis occurs, etc. The most important factor among them is the redox composition of the initial solution, which was previously shown [21–23] to define the combustion conditions and temperature in the reaction zone. Despite much research [10,24,25] being focused on obtaining lanthanum orthoferrite by solution combustion synthesis, the influence of redox composition on processes of $LaFeO_3$ nanocrystal formation has not been studied in detail. Thus, the theoretical and practical goals of the present paper are the investigation of the

influence of redox composition on $LaFeO_3$ formation and synthesis of lanthanum orthoferrite nanopowders with a high specific surface area.

2. Experimental

2.1. Materials synthesis

The compositions based on $LaFeO_3$ were prepared by the solution combustion synthesis. The details of synthesis procedure have been previously described [26]. As starting materials, lanthanum and iron nitrates and glycine were used. All starting materials were analytic-grade purity. Lanthanum and iron nitrates were taken in a stoichiometric ratio according to the following reaction:

$$3La(NO_3)_3 + 3Fe(NO_3)_3 + 10C_2H_5NO_2 = 3LaFeO_3 + 14N_2 + 20CO_2 + 25H_2O,$$

while the amount of glycine was varied towards to the total amount of nitrates (G/N) from 0.1 to 1.4. G/N ratio was calculated as follows:

$$G/N = \frac{n_{gly}}{n'_{NO_3^-} + n''_{NO_3^-}},$$

where n_{gly} – moles of glycine, $n'_{NO_3^-}$ and $n''_{NO_3^-}$ – moles of lanthanum and iron nitrates, correspondingly. Nitrates of iron and lanthanum and glycine were dissolved in distilled water under a vigorous stirring. Then, the solution was heated until water evaporation that caused the transition of solution into gel followed by its spontaneous ignition. The product of glycine-nitrate synthesis is foam-like substance, which becomes a brown powder after milling in a mortar.

2.2. Materials characterization

The prepared samples were characterized by the following techniques. Powder X-ray diffraction (PXRD) performed on a Rigaku SmartLab 3 diffractometer was used to identify the crystalline phases and estimate the average crystallite size and the crystallite size distribution. The Scherrer equation was used for crystallite size calculation. The fundamental parameters approach, which is implemented in standard Rigaku software supplied to the diffractometer, was used to find the crystallite size distribution. Scanning electron microscopy (SEM) with energy dispersive X-ray analysis (EDX) performed on a Tescan Vega 3 microscope was employed to characterize morphology and elemental composition. The specific surface area was measured by Brunauer–Emmett–Teller (BET) method using N_2 as adsorbed gas on an Micromeritics ASAP 2020 instrument. The density of the samples was determined with a helium pycnometer (Micrometrics AccuPyc 1330). The thickness of interpore partition was calculated from pycnometric density and specific surface area data in an approximation of an infinite plate of finite thickness [27,28] according to the following formula:

$$h = \frac{2}{S \cdot \rho},$$

where h – average interpore partition, S – specific surface area and ρ – density of the sample.

3. Results and discussion

According to EDX analysis, the lanthanum to iron ratio in all obtained powders answers to 1:1 ratio given by synthesis procedure within the method error. The phase composition of the powders evaluated from PXRD drastically differed, depending on G/N ratio. For instance, when the starting solution contains considerable excess or shortage of glycine (G/N = 1.2, 1.4 or G/N = 0.1, 0.2) the final solid products are completely or almost amorphous (Fig. 1). In the case of G/N ratio lying in between these edge points the crystalline phase of $LaFeO_3$ with orthorhombic structure is predominantly found in the final solid products (Fig. 1). Phase analysis is presented in details in Fig. 2(a). The data demonstrate that as G/N ratio comes closer to the stoichiometric point (G/N = 0.6) the amount of amorphous phase decreases to zero. It is worth noting that at G/N = 0.2, in addition to the amorphous phase, a trace amount of $La(OH)_2NO_3$ crystalline phase is present. In the similar system based on $YFeO_3$, the impurities of nitrate derivatives of REE were also found in the powders obtained by glycine-nitrate synthesis at non-stoichiometric G/N ratios, but their crystallization did not occur during combustion [29]. In the case of $LaFeO_3$ system, the formation of $La(OH)_2NO_3$ is probably explained by a higher temperature in the reaction zone in comparison to that which can be implemented during synthesis in the $YFeO_3$ system. The higher temperature, in turn, can be rationalized to be due to the catalytic effect of the formed $LaFeO_3$ on the combustion process which leads to an acceleration of energy release and even when G/N ratio is far from stoichiometric, sufficient temperatures are reached in the system to cause the crystallization of lanthanum nitrate derivatives.

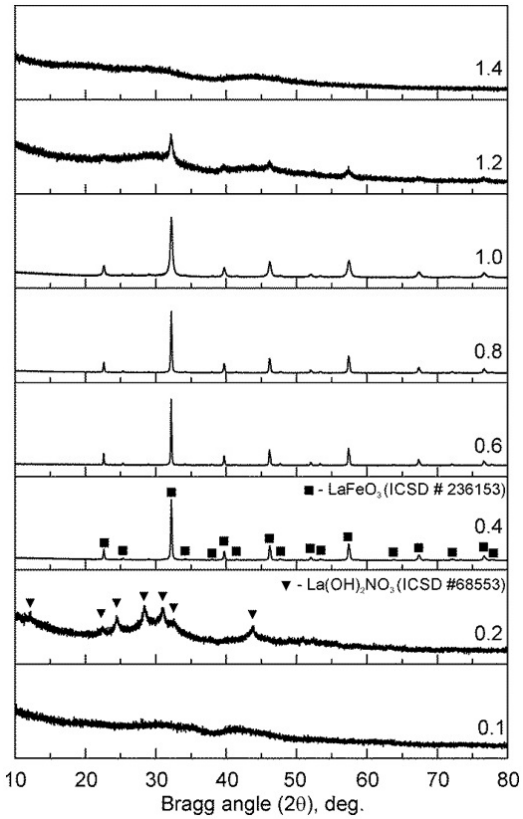

FIG. 1. X-ray diffraction patterns of products of $LaFeO_3$ glycine-nitrate synthesis obtained at different G/N ratios

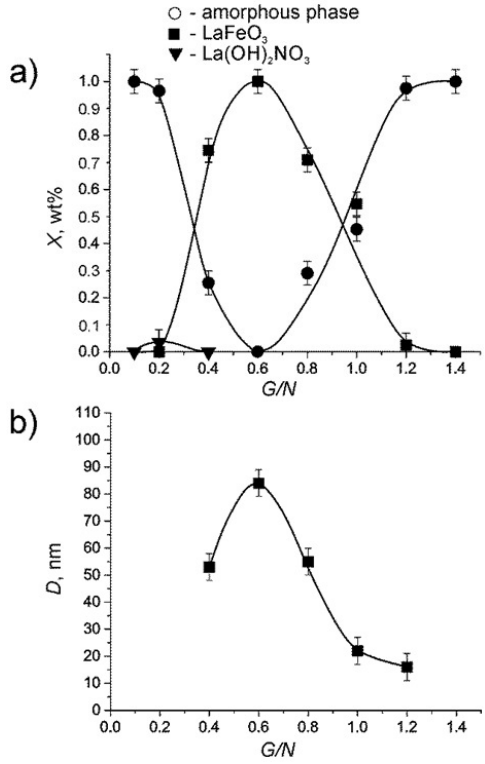

FIG. 2. Phase composition of glycine-nitrate synthesis products (a) and $LaFeO_3$ average crystallite size (b) depending on G/N ratio

The typical dependence of phase composition on G/N ratio (Fig. 2(a)), as was previously shown for the similar system [21], is connected with the dependence of temperature on this parameter. The temperature in the reaction zone is considered to be maximum at the stoichiometric point and decreases both towards the excess and the shortage of glycine. Therefore the most stable and defect-free crystalline phases are conventionally formed at the stoichiometric G/N ratio.

This trend is also noted in the dependence of the average crystallite size on the G/N ratio (Fig. 2), as far as at the stoichiometric point it usually reaches the maximum value and in the considered system the value is about 85 nm. For comparison, the average crystallite size reaches only about 50 nm in the $YFeO_3$ system. This considerable difference can also be explained by the catalytic activity of $LaFeO_3$ and higher temperature that intensify the recrystallization processes in the reaction zone and leads to the growth of the lanthanum orthoferrite nanocrystals. In other respects, the dependence of the average crystallite size on glycine-nitrate ratio repeats those known for other systems [21,26]. The samples obtained at G/N ratio of 0.4 and 0.8 have almost the same average crystallite size of about 55 nm. The powder with the smallest average crystallite size of about 20 nm and mostly consisting of crystalline $LaFeO_3$ was obtained at G/N = 1.0. At the same time, this sample is characterized by the narrowest shape of crystallite size distribution among other samples and the size of crystallite majority lies in the range of 10 – 35 nm (Fig. 3). The broadest crystallite size distribution, as it was expected, belongs to the sample obtained at stoichiometric G/N ratio and its crystallite size is varied from 50 to 110 nm. The sample obtained at G/N = 1.2 despite on the smallest size of crystallites is excluded from consideration as it contains an only trace amount of $LaFeO_3$. Thus, from a practical point of view, the lanthanum orthoferrite nanocrystals obtained at G/N = 1.0 are the most interesting since they have the smallest crystallite size and the narrowest crystallite size distribution among the whole set of samples, what meets important requirements for nanopowders using as a basis for magnetic and electric materials [4,5].

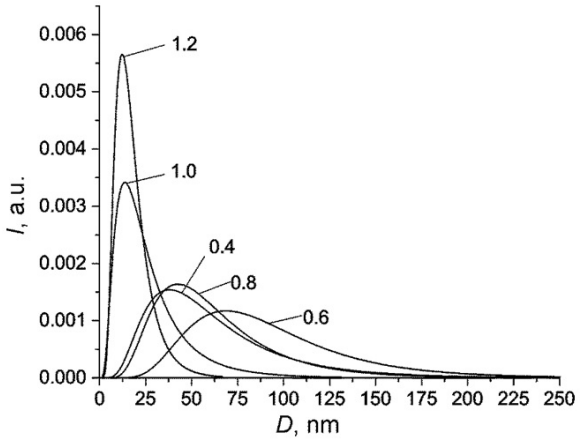

FIG. 3. Size distribution of $LaFeO_3$ nanocrystals obtained at different G/N ratios

Another practically important parameter of the obtained $LaFeO_3$ nanocrystals and compositions on their basis is the specific surface area. The results of measurements of the specific surface area are shown in Fig. 4(a). According to the shown data, the samples synthesized at a glycine-nitrate ratio close to the stoichiometric point (G/N = 0.4 – 0.8) have a relatively low specific surface area of about 10 m^2/g, which agrees with data reported previously [10,24]. At G/N below 0.4, a drastic decrease of the specific surface area to 0.5 m^2/g (G/N = 0.1) is observed, which is related to the replacement of the bulk combustion mode inherent to the stoichiometric reaction by the smoldering mode. The smoldering mode is characterized by relatively low temperatures in the reaction zone and low reaction rate that promotes the formation of several by-products ($La(OH)_2NO_3$ and others) in the reaction and a poorly developed surface for the products. On the contrary, as G/N ratio exceeds stoichiometric value a dramatic increase of specific surface area to 33 m^2/g is observed (G/N = 1.0), which can be explained by an increase of waste gases and maintaining enough high temperature at the same time. Thus, it was shown the possibility to increase the specific surface area of nanocrystalline $LaFeO_3$ by facile varying of redox composition of the initial solution, which was previously reached only by additional modification of glycine-nitrate synthesis [25]. Helium pycnometry data provide evidence for the high purity of obtained lanthanum orthoferrite nanocrystals, as the value of the pycnometric density of samples synthesized at G/N = 0.4 – 1.0 almost matches with the X-ray density ($\rho^{XRD}_{LaFeO_3} = 7.081$ g/cm^3) of orthorhombic $LaFeO_3$ (Fig. 4(b)). However, as in the case of excess of

nitrates ($G/N < 0.4$), so in the case of their deficiency ($G/N > 1.0$) in the reaction mixture, the by-products of redox reaction such as nitrate and carbonate derivatives of iron and lanthanum reduce the pycnometric densities of the samples. The agreement between the average crystallite size of $LaFeO_3$ and the average thickness of interpore partition of foam-like samples (Fig. 5) within the limits of experimental error for the broad G/N range of 0.4 – 1.0 (Fig. 2(b) and Fig. 4(c)), as well as similar shape of dependence of these values on G/N argue that interpore partition is formed by layers of $LaFeO_3$ nanocrystals and thickness of the layers is comparable with the average crystallite size. Herewith, according to SEM data (Fig. 5), the morphology and the microstructure parameters of the glycine-nitrate synthesis products corroborate conclusions stated above about the influence of the glycine-nitrate ratio on the formation of nanocrystalline $LaFeO_3$. Thus, the sample obtained at G/N = 0.1 (Fig. 5(a)) is a dense low-porosity substance of micron size, which has an extremely low specific surface area and a large thickness of interpore partition. While the sample obtained at stoichiometric G/N ratio (Fig. 5(b)) already has rather developed porosity structure, but the thickness of interpore partition is still large enough ($\sim$100 nm). As opposed to the previous cases, synthesis at a G/N ratio = 1.0 leads to the formation of the sample with the most developed porosity and surface (Fig. 5(c)), the major bulk of which is formed by $LaFeO_3$ nanocrystals with the size of 20–25 nm. This peculiar structure of the product of glycine-nitrate synthesis – nanocrystals of lanthanum orthoferrite – allows one to suppose the successful application of materials based on the nanocrystals for photocatalysis. The assumption seems to be especially reasonable since successful results have been obtained elsewhere [11]. Finally, at G/N = 1.4 (Fig. 5(d)), i.e. in a large excess of glycine, the sample obtained was of micron size and with high porosity and specific surface. However, a considerable part of the sample consists of combustion by-products (mainly carbonate derivatives of iron and lanthanum), which was confirmed by the extremely low pycnometric density and the great fraction of the amorphous phase in the composition.

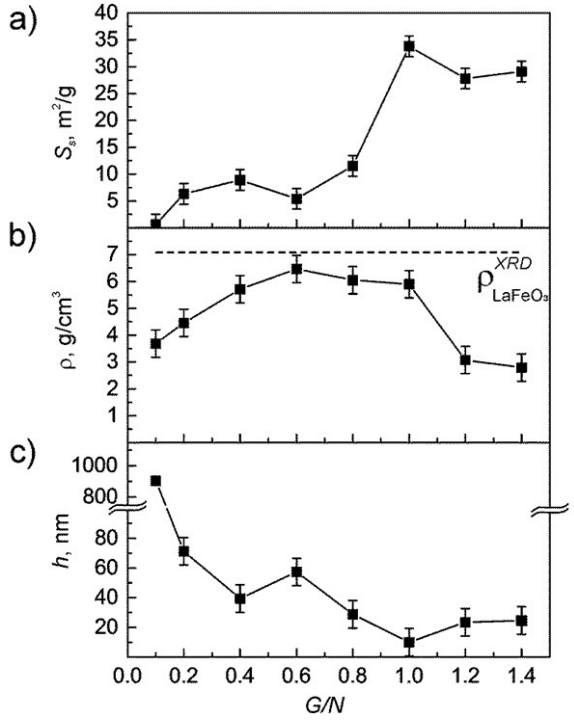

FIG. 4. Specific surface S_s (a), pycnometric density ρ (b) and thickness of interpore partition h (c) of glycine-nitrate combustion products depending on G/N ratio. Dashed line – X-ray density of orthorhombic $LaFeO_3$, equal to 7.081 g/cm^3

Thus, in this paper, the possibility of nanocrystalline lanthanum orthoferrite synthesis from glycine and nitrate precursors was demonstrated. Additionally, it was also shown that by varying the glycine-nitrate composition of the initial solution, one can vary the selected properties of the obtained nanocrystals. Samples were obtained based on $LaFeO_3$ nanocrystals with different microstructure and the average crystallite size, ranging from 18$\pm$2 to 85$\pm$9 nm, which provided nanopowders with specific surface area values ranging from 8 – 33 m^2/g. It was established that in the broad range of G/N ratio 0.4 – 1.0, high-porosity samples are mainly formed by nano-scale

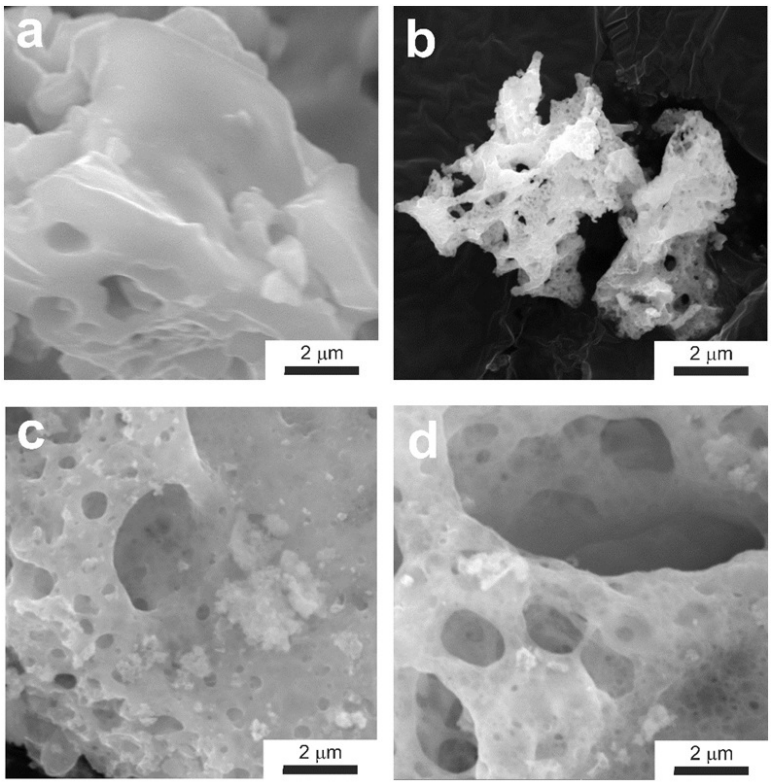

FIG. 5. SEM images of glycine-nitrate combustion products obtained at 0.1 (a), 0.6 (b), 1.0 (c) and 1.4 (d) G/N ratio

single crystal layers of $LaFeO_3$, the thickness of which is comparable with the average crystallite size, making these nanocrystalline powders promising candidates for catalytic materials.

Acknowledgments

The reported study was funded by RFBR, according to the research Project No. 16-33-00345. The powder X-ray diffraction and SEM studies were performed on equipment of the Engineering Center of the Saint-Petersburg State Technological Institute (Technical University).

References

[1] Pavlovska O.B., Vasylechko, Lutsyuk I. V., Koval N.M., Zhydachevskii Y.A., Pienižek A. Structure Peculiarities of Micro- and Nanocrystalline Perovskite Ferrites $La_{1-x}Sm_xFeO_3$. *Nanoscale Res. Lett.*, 2017, **12**, P. 153–159.

[2] Ciambelli P., Cimino S., De Rossi S., Lisi L., Minelli G., Porta P., Russo G. $AFeO_3$ (A=La, Nd, Sm) and $LaFe_{1-x}Mg_xO_3$ perovskites as methane combustion and CO oxidation catalysts: structural, redox and catalytic properties. *Appl. Catal. B: Environ.*, 2001, **29**(4), P. 239–250.

[3] Wang J., Liu Q., Xue D., Li F. Synthesis and characterization of $LaFeO_3$ nano particles. *J. Mater. Sci. Lett.*, 2002, **21**(13), P. 1059–1062.

[4] Rajendran M., Bhattacharya A.K. Nanocrystalline orthoferrite powders: Synthesis and magnetic properties. *J. Eur. Ceram. Soc.*, 2006, **26**(16), P. 3675–3679.

[5] Khetre S.M., Jadhav H.V., Jagadale P.N., Kulal S.R., Bamane S.R. Studies on electrical and dielectric properties of $LaFeO_3$. *Adv. Appl. Sci. Res.*, 2011, **2**(4), P. 503–511.

[6] Markova-Velichkova M., Lazarova T., Tumbalev V., Ivanov G., Kovacheva D., Stefanov P., Naydenov A. Complete oxidation of hydrocarbons on $YFeO_3$ and $LaFeO_3$ catalysts. *Chem. Eng. J.*, 2013, **231**, P. 236–244.

[7] Lomanova N.A., Pleshakov I.V., Volkov M.P., Gusarov V.V. Magnetic properties of Aurivillius phases $Bi_{m+1}Fe_{m-3}$ Ti_3O_{3m+3} with m =5.5, 7, 8. *Mater. Sci. Eng. B.*, 2016, **214**, P. 51–56.

[8] Popkov V.I., Almjasheva O.V., Semenova A.S., Kellerman D.G., Nevedomskyi V.N., Gusarov V.V. Magnetic properties of $YFeO_3$ nanocrystals obtained by different soft-chemical methods. *J. Mater. Sci. Mater. Electron.*, 2017, **28**(10), P. 7163–7170.

[9] Nguyen A.T., Nguyen T.D., Mittova V.O., Berezhnaya M.V., Mittova I.Y. Phase composition and magnetic properties of $Ni_{1-x}Co_xFe_2O_4$ nanocrystals with spinel structure, synthesized by Co-precipiation. *Nanosyst. Physics, Chem. Math.*, 2017, **8**(3), P. 371–377.

[10] Parida K.M., Reddy K.H., Martha S., Das D.P., Biswal N. Fabrication of nanocrystalline $LaFeO_3$: An efficient sol–gel auto-combustion assisted visible light responsive photocatalyst for water decomposition. *Int. J. Hydrogen Energy.*, 2010, **35**(22), P. 12161–12168.

[11] Acharya S., Padhi D.K., Parida K.M. Visible light driven $LaFeO_3$ nano sphere/RGO composite photocatalysts for efficient water decomposition reaction. *Catal. Today.*, 2017, P. 1–12.

[12] Iervolino G., Vaiano V., Sannino D., Rizzo L., Palma V. Enhanced photocatalytic hydrogen production from glucose aqueous matrices on Ru-doped $LaFeO_3$. *Appl. Catal. B Environ.*, 2017, **207**, P. 182–194.
[13] Tien N.A., Mittova I.Y., Almjasheva O.V., Kirillova S.A., Gusarov V.V. Influence of the preparation conditions on the size and morphology of nanocrystalline lanthanum orthoferrite. *Glas. Phys. Chem.*, 2008, **34**, P. 756–761.
[14] Van Tac D., Mittova V.O., Mittova I.Y. Influence of Lanthanum Content and Annealing Temperature on the Size and Magnetic Properties of Sol – Gel Derived $Y_{1-x}La_xFeO_3$ Nanocrystals. *Inorg. Mater.*, 2011, **47**(5), P. 590–595.
[15] Zheng W., Liu R., Peng D., Meng G. Hydrothermal synthesis of $LaFeO_3$ under carbonate-containing medium. *Mater. Lett.*, 2000, **43**(1-2), P. 19–22.
[16] Ji K., Dai H., Deng J., Song L., Xie S., Han W. Glucose-assisted hydrothermal preparation and catalytic performance of porous $LaFeO_3$ for toluene combustion. *J. Solid State Chem.*, 2013, **199**, P. 164–170.
[17] Tugova E.A., Karpov O.N. Nanocrystalline perovskite-like oxides formation in Ln_2O_3- Fe_2O_3-H_2O (Ln = La, Gd) systems. *Nanosyst.: Physics, Chem. Math.*, 2014, **5**(6), P. 854–860.
[18] Nguyen A.T., Knurova M.V, Nguyen T.M., Mittova V.O., Mittova I.Y. Synthesis and the study of magnetic characteristic of nano $La_{1-x}Sr_xFeO_3$ by co-precipitation method. *Nanosyst.: Physics, Chem. Math.*, 2014, **5**(5), P. 692–702.
[19] Cherepanov V.A., Gavrilova L.Y., Volkova N.E., Urusov A.S., Aksenova T.V, Kiselev E. Phase equilibria and thermodynamic properties of oxide systems on the basis of rare earth, alkaline earth and 3d-transition (Mn, Fe, Co) metals. A short overview of, *Chim. Techno Acta.*, 2015, **2**(4), P. 273–305.
[20] Wang J., Dong X., Qu Z., Liu G., Yu W. Electrospinning Preparation of $LaFeO_3$ *Nanofibers, Mod. Appl. Sci.*, 2009, **3**(9), P. 65–71.
[21] Popkov V.I., Almjasheva O.V. Yttrium orthoferrite $YFeO_3$ nanopowders formation under glycine-nitrate combustion conditions. *Russ. J. Appl. Chem.*, 2014, **87**(2), P. 167–171.
[22] Varma A., Mukasyan A.S., Rogachev A.S., Manukyan K.V. Solution Combustion Synthesis of Nanoscale Materials. *Chem. Rev.*, 2016, **116**(23), P. 14493–14586.
[23] Khaliullin S.M., Zhuravlev V.D., Bamburov V.G. Solution-combustion synthesis of oxide nanoparticles from nitrate solutions containing glycine and urea: Thermodynamic aspects. *Int. J. Self-Propagating High-Temperature Synth.*, 2016, **25**(3), P. 139–148.
[24] Kondakindi R.R., Karan K., Peppley B.A. A simple and efficient preparation of $LaFeO_3$ nanopowders by glycine–nitrate process: Effect of glycine concentration. *Ceram. Int.*, 2012, **38**(1), P. 449–456.
[25] Komova O.V., Simagina V.I., Mukha S.A., Netskina O.V., Odegova G.V., Bulavchenko O.A., Ishchenko A.V., Pochtar' A.A. A modified glycine–nitrate combustion method for one-step synthesis of $LaFeO_3$. *Adv. Powder Technol.*, 2016, **27**(2), P. 496–503.
[26] Zaboeva E.A., Izotova S.G., Popkov V.I. Glycine-nitrate combustion synthesis of $CeFeO_3$-based nanocrystalline powders. *Russ. J. Appl. Chem.*, 2016, **89**(8), P. 1228–1236.
[27] Popkov V.I., Almjasheva O.V., Nevedomskiy V.N., Sokolov V.V., Gusarov V.V. Crystallization behavior and morphological features of $YFeO_3$ nanocrystallites obtained by glycine-nitrate combustion, *Nanosyst.: Physics, Chem. Math.*, 2015, **6**(6), P. 866–874.
[28] Popkov V.I., Almjasheva O.V., Schmidt M.P., Izotova S.G., Gusarov V.V. Features of nanosized $YFeO_3$ formation under heat treatment of glycine–nitrate combustion products Russ. *J. Inorg. Chem.*, 2015, **60**(10), P. 1193–1198.
[29] Wang X.J., Shen H.Y., Tian H.Y., Yang Q.H. Photocatalytic Degradation of Water-Soluble Azo Dyes by $LaFeO_3$ and $YFeO_3$. *Adv. Mater. Res.*, 2012, **465**, P. 37–43.